Proceedings of The Fourteenth (2004) International Offshore and Polar Engineering Conference
Toulon, France, May 23–28, 2004

ISBN 1-880653-62-1 (Set); ISSN 1098-6189 (Set)

Electromagnetic-inductive Measurements for the Undeformed and Deformed Sea-ice and Snow in the East Antarctic

Kazutaka Tateyama
Sea Ice Research Laboratory, Institute of Low Temperature Science, Hokkaido University
Mombetsu, Hokkaido, Japan
Shotaro Uto
National Maritime Research Institute
Mitaka, Tokyo, Japan
Kunio Shirasawa
Sea Ice Research Laboratory, Institute of Low Temperature Science, Hokkaido University
Mombetsu, Hokkaido, Japan
Hiroyuki Enomoto
Department of Civil Engineering, Kitami Institute of Technology
Kitami, Hokkaido, Japan

ABSTRACT

Indirect ice and snow thickness measurements were carried out for the winter and spring Antarctic sea ice by using the electromagnetic-inductive (EMI) device on the East Antarctic pack ice area. This study investigated the effect of saline slush snow layer over the sea ice and seawater-filled gap to the snow and sea ice thickness measured by EMI. A result shows underestimations of EMI thickness, which might be caused by high conductive seawater-filled gaps between ice floes, appeared on thicker ice over 3.5 m. This study improved the validity of applying a multi-rafted ice model for these ice conditions.

KEY WORDS: Sea-ice, thickness, electromagnetic-inductive measurement, Antarctic

INTRODUCTION

Antarctic Remote Ice Sensing Experiment 2003 (ARISE 2003) was conducted in the Antarctic seasonal ice-covered area where is 115-120^{o}E and 64-65^{o}S between September and October of 2003, as a part of Voyage 1 cruse of RSV Aurora Australis. The purpose of the experiment is to validate reliability and accuracy of the satellite passive microwave radiometer; Advanced Microwave Scanning Radiometer (AMSR) and AMSR-E in measuring of sea ice products. We collected ground truth data from the ice floes in order to improve and develop algorithms providing ice concentration, thickness and snow depth. Measurements of ice thickness were carried out by the helicopter-borne, ship-borne and ground-based electromagnetic-inductive (EMI) devices. The authors took part in the ground-based EMI measurements in conjunction with measurements of sea ice thickness, snow depth, surface radiative temperature and salinity of snow and ice.

The EMI devices have been used for detecting changes in the earth conductivity, such as underground metal deposits. The EMI sensor measures the terrain conductivity, which is derived from a quadrature component of the ratio of the secondary to the primary electromagnetic field under the operation of the low value of induction number.

Recently, EMI measurements have been employed to indirect measurement of sea ice thickness without drilling or breaking up by a helicopter and an ice-breaker (Kovacs et al., 1987; Multala et al., 1996; Haas et al., 1997; Worby et al., 1999; Uto et al., 2002; Reid et al., 2003). Sea ice thickness can be determined by utilizing the large contrast in the electrical conductivity between sea ice (<80mS/m) and seawater (2400mS/m) (Kovacs et al., 1987). A method to calculate sea ice and snow thickness from EMI apparent conductivity for the Arctic and Antarctic sea ice by using a 1-D multi-layers model was introduced by Haas et al. (1997) and Haas (1998).

This study reports the results of evaluation of EMI sounding to observe snow and sea ice thickness on winter and spring Antarctic pack ice area as shown in Fig.1. The purpose of this study is to assess the 1-D multi-layers model, which is constructed from ice core data, to understand the applicability of EMI measurement for the various sea ice conditions.

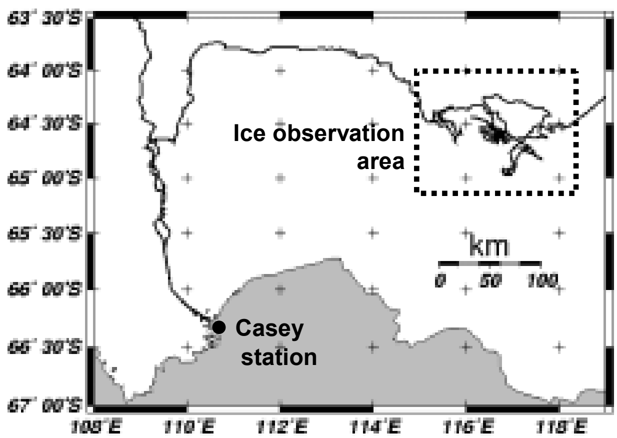

Fig. 1 Map of the ARISE 2003 expedition in the East Antarctic. The

thick line shows the cruise track. The dotted-line section indicates the ice observation area.

METHOD

Measurements

The ground based EMI instrument utilized in this study is an EM-31/ICE (*Geonics Co., Ltd., Canada*), having one pair of a transmitter coil (Tx) and a receiver coil (Rx). This instrument is widely used for measurement of sea ice thickness [Kovacs and Morey, 1991; Haas et al., 1997; Worby et al., 1999; Uto et al., 2002]. The operating frequency is 9.8 kHz and the distance between Tx and Rx is 3.66m. The apparent footprint diameters for a vertical coplanar (VCP) mode and a horizontal coplanar (HCP) mode are, respectively, between 1.25 to 1.35 and 3.7 to 3.8 times the instrument heights above the interface between ice bottom and seawater (Kovacs et al., 1995).

Measurements of ice thickness and snow depth were made for 13 transects of the length from 50 to 500m on 10 different ice floes. EMI and drill-hole observations were made at the intervals of 1 to 4 m, and 1 to 2 m, respectively. We measured apparent conductivity σ_a and in-phase by VCP and HCP modes. In this study we focused the VCP apparent conductivity, since the VCP mode has a finer footprint than the HCP mode and is suitable for thinner ice.

The ice thickness and snow depth ranged from 0.2 to over 4 m and from 0.04 to 1m, respectively. Surface topography was also measured by a laser distance meter. Ice cores were taken at 50 m interval. These ice cores were made holes at 5 cm interval and then ice temperature was measured by a thermister in the ice core hole. After that ice cores were cut into 5cm sections for melting and measuring salinity. Snow pit works were also carried out at 50 m interval. Snow density, temperature, salinity, type, crystal size and wetness were measured. Seawater conductivity (σ_W) was measured by the ship's sensor.

EM-31/ICE cannot distinguish the difference between snow and ice. Therefore, we discuss the relationship between the apparent conductivities derived from EMI measurements and observed snow and ice thickness.

Modeling

First, we calculated the sea ice conductivity σ_I from ice core data. According to the Archie's law (Archie, 1942), σ_I can be calculated from brine volume V_b and conductivity σ_b.

$$\sigma_I = \sigma_b V_b^m \quad (1)$$

We used the value of m = 1.75 according to Haas (1997). The σ_b was calculated by the following equation (Stogryn and Desargant, 1985),

$$\sigma_b = -T\exp(0.5193+0.08755T) \quad (-22.9°C \leq T \leq -0.5°C) \quad (2)$$

where, T is the physical temperature of sea ice. The brine volume was calculated by Frankenstein and Garner (1967) as the following equation (3).

$$V_b = S(49.185/\text{abs}(T)+0.532) \quad (-22.9°C \leq T \leq -0.5°C) \quad (3)$$

Those calculations were carried out for each 5cm section of ice cores. The bulk sea ice conductivity σ_{Ibulk} was calculated by averaging σ_I profile for each individual ice core. Table 1 indicates a summery of ice core analysis.

Figure 2 shows the relationship between the core length and bulk sea ice conductivity σ_{Ibulk} for the all core samples. Thinner ice (<0.5m) showed higher values and larger scatters in the conductivity ranged from 60 to 160 mS/m. In this study, higher scattering seems to decrease over about 0.5 m thick. Therefore, we used the mean bulk ice conductivity as σ_{Ibulk} = 46.43 ms/m for more than 0.5 m thick ice and mean seawater conductivity below sea ice as σ_W = 2765 mS/m for calculating multi-layer model. The conductivities of air and snow (σ_{AIR}, σ_S) are used as 0 mS/m.

Table 1. The properties of ice core. T_{Ibulk}, S_{Ibulk}, H, V_b, σ_{ibulk}, σ_W mean bulk ice temperature, bulk salinity, thickness, brine volume, bulk ice conductivity and seawater conductivity.

	T_{Ibulk} [°C]	S_{Ibulk} [‰]	H [cm]	V_b [%]	σ_{Ibulk} [mS/m]	σ_W [mS/m]
Min	-6.39	4.44	20.0	3.17	24.61	2753
Max	-2.24	8.96	269.0	6.42	158.55	2770
Ave all	-3.76	6.41	95.9	4.58	67.28	2765
Ave >50cm	-3.20	5.65	129.5	4.04	46.43	2765

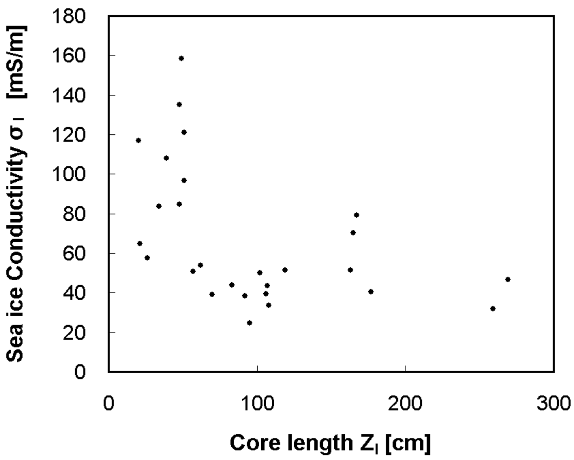

Fig. 2 The relationship between core length and sea ice conductivity.

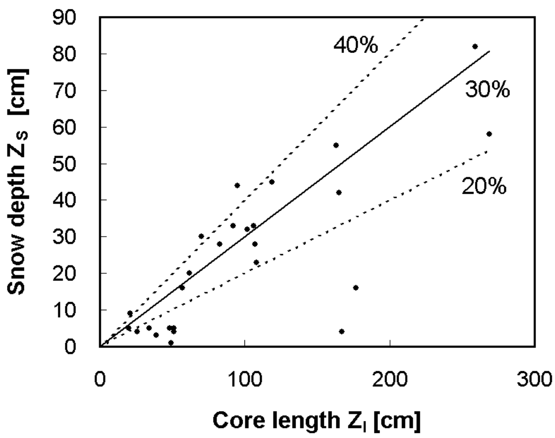

Fig. 3 The relationship between core length and snow depth. Lines of 20%, 30% and 40% mean the ratios of snow depth to ice core length.

Figure 3 shows the relationship between ice core length and snow depth. As the rate of the snow depth to the ice core length was 30% ±10%, we assumed the snow depth was 30% of the ice thickness for model calculation. In addition, as the snow depth did not exceed 0.8 m in this observation, 0.8 m was used as the maximum value for model calculation.

We used the program PCLOOP provided by the Geonics (McNeill, 1980) as a 1-D multi-layer model for calculating apparent conductivity σ_a from ice thickness (Z_I), snow depth (Z_S), σ_I, σ_W and instrument height over the snow surface (Z_L).

$$\sigma_a = f(Z_I, Z_S, Z_L, \sigma_I, \sigma_W) \quad (4)$$

First, we set a 1-D three layers model, which is consisted of snow layer, ice layer and seawater layer. Parameters of 1-D three layers model in this study is summarized as shown in Fig.4.

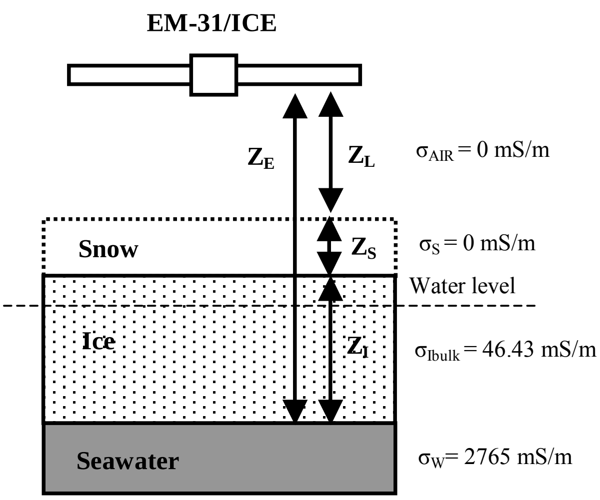

Fig.4 1-D three layers model in this study. The air conductivity σ_{AIR} and snow conductivity σ_S were set to be 0 mS/m. Z_E, Z_L, Z_S and Z_I are the distances between EM-31/ICE and ice bottom, EM-31/ICE and snow surface, snow depth and ice thickness, respectively.

We used two different constant heights Z_L when we carried out EMI measurement on the ice floes in this study. When snow surface is hard enough to walk on, measurements were conducted at 0.84 m height from snow surface to the center of a receiver coil, which was the height of the investigator's shoulder. On the other hand, when snow was soft, the instrument was put on the snow surface at the 0.11 m height.

The σ_a can be calculated from field measurements and ice core analysis by PCLOOP (Eq. (4)). Hence, the following exponential regression curves were determined by the least-mean square fitting of the calculated data.

$$Z_E = 0.242 + 4.365\exp(-\sigma_a/305.417) + 17.264\exp(-\sigma_a/26.718) \quad (5)$$

$$Z_E = 0.853 + 4.639\exp(-\sigma_a/181.227) + 17.430\exp(-\sigma_a/43.027) \quad (6)$$

where Z_E is the distance between EM-31/ICE and ice bottom. Eq. (5) is for Z_L = 0.11 m, and Eq. (6) for Z_L = 0.84 m. The sum of ice thickness and snow depth can be calculated by (Z_E - Z_L). As Z_L are constant in this study, the variability of Z_E shows the variability of snow and ice thickness.

Figure 5 shows modeled curves of the relationship between apparent conductivity and ice thickness derived from Eq. (5) and (6). Those exponential fitting lines show 99% explain of each total variance. This result suggested that apparent conductivity at Z_L = 0.84 m showed relatively higher values than that of Z_L = 0.11 m in the thinner ice less than 1 m. The model of Z_L = 0.11 m should indicate more adequate values than that of Z_L = 0.84 m, because this difference is caused by the lack of thinner ice data for the model of Z_L = 0.84 m. As the difference in the models for both heights is not significant, within ±5%, we can neglect the effect of the difference between those instruments heights and use the model of Z_L = 0.11 m.

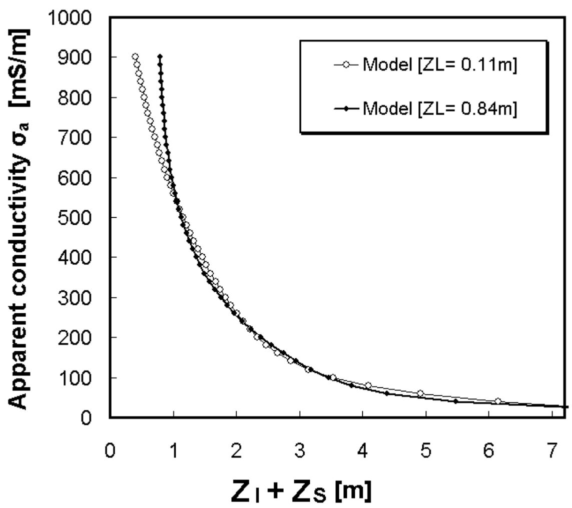

Fig. 5 Modeled sea ice and snow thicknesses at Z_L = 0.11 m and 0.84 m calculated from Eq. (5) and (6) versus apparent conductivity.

RESULTS AND DISCUSSIONS

First, we compared the model curve from our 1-D model with previous study's model. Figure 6 shows the comparison of modeled curves obtained from this study with that from summer Arctic ice (Eicken et al., 2001). They reported a modeled curve derived from mean ice and water conductivities for Arctic summer condition by ground-based measurements in SHEBA sites. The model curve obtained by Eicken et al. indicates a good agreement generally, but also showed underestimation of Z_E from σ_a as compared with this study. This difference is caused not only by higher value σ_I = 58 mS/m and lower value of σ_W = 2450 mS/m for summer Arctic Sea than this study for winter and spring Antarctic Sea, but also the existence of relative fresh melt water on/underneath ice. This low conductive water contributes overestimation of ice thickness (Eicken et al., 2001).

Figure 7 shows the result on the relationship between Z_E and σ_a at (a) Z_L=0.11m and (b) Z_L=0.84m for this study. Z_E data were derived by averaging drilling thickness and snow depth horizontally for 4m, which is typical footprint size of VCP mode. These figures show that the model agrees generally with in-situ Z_E, but Z_E was overestimated in less than 0.7m. EMI measurement indicates doubtful results in this shallower range. Kovacs and Morey (1991) suggested that the ice thickness or distance to the ice-water interface, of less than about 0.7m cannot be measured within ±10% of true distance when an EM-31/ICE stays on the snow or ice surface. As this problem is caused by the characteristic of instrument, it can be settled by elevating the

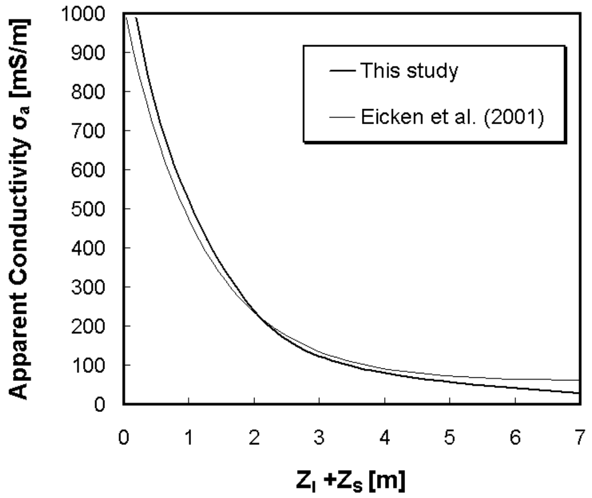

Fig. 6 Comparison of modeled curves on the (Z_I+Z_S) $-\sigma_{a)}$ relationship between this study and Eicken et al. (2001).

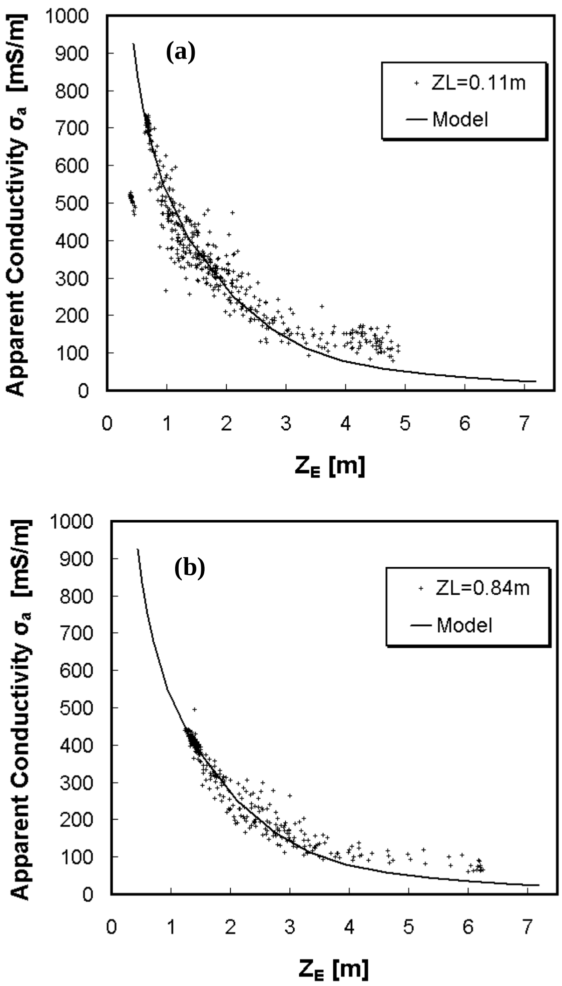

Fig. 7 Z_E-σ_a relationship at (a) Z_L=0.11m and (b) Z_L=0.84m for the ground-based EMI measurement in the east Antarctica.

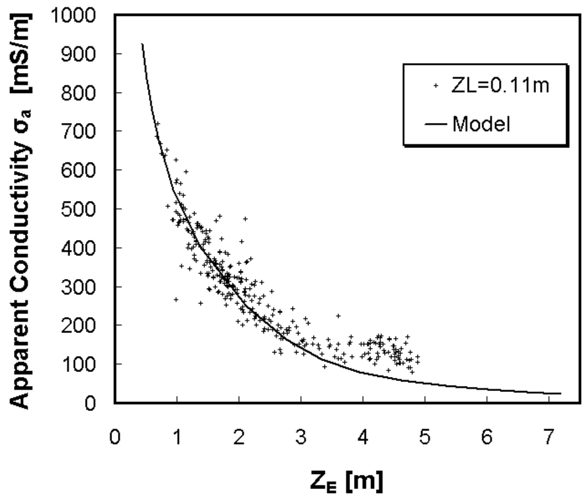

Fig. 8 Z_E-σ_a relationship without thinner ice data less than 0.7m thick at Z_L=0.11m.

instrument 0.7 m or more (Kovacs and Morey, 1991). Therefore we eliminated data, which indicate less than 0.7 m thick, from data processing for observation at Z_L=0.11m. The result showed in Fig. 8.

For observation at Z_L=0.84 m, less than 0.7 m thick data do not exist. From Fig.7 (b) and Fig.8, model curves showed fairly good agreement with data less than 3.5 m, but thicker ice more than 3.5 m indicated that model underestimates Z_E and a large scattering, especially on the plot of Z_L = 0.11m. These results suggested that the limitation of distance between the EMI instrument and ice bottom for sea ice measurement seems to be 3.5 m.

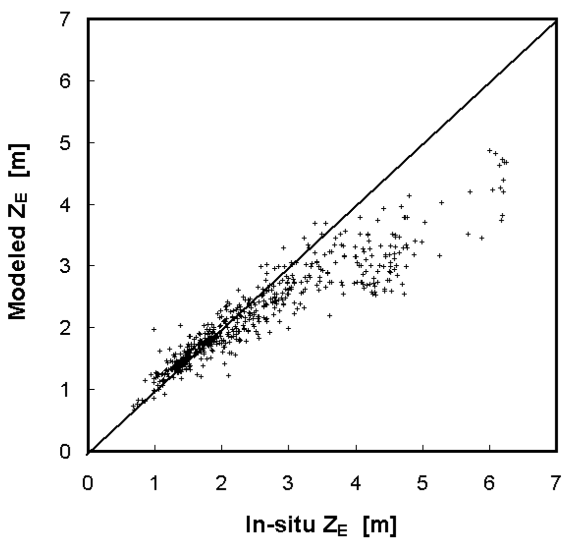

Fig. 9 Comparison between in-situ and modeled Z_E.

Figure 9 shows the comparison between modeled and in-situ Z_E. Modeled Z_E was calculated from observed σ_a. The model indicated a good agreement with thinner ice less than 3.5 m, on the other hand, the model showed underestimation obviously in thicker ice more than 3.5 m. The correlation coefficient between in-situ and modeled Z_E is 0.90.

Kovacs and Morey (1991) reported that EM-31/ICE can be used to determine sea ice and snow thickness from about 0.7 to 5 m, within an accuracy of ±10% of in-situ thickness. They also discussed about a significant decrease in correlation for thicker ice more than 3.5 m, and referred that this poor agreement between EM-31/ICE and drill-hole measurements is attributable to the highly variable ice/water interface such as seawater-filled, because ice and snow thickness over 3.5 m were obtained in areas of deformed ice. They used two regression curves to represent through the data at 3.5 m as a break point.

Haas (1998) also suggested that this kind of underestimation cannot be explained by increasing ice and water conductivity in the multi-layer model, instead, it can be caused by existence of slush, which is wet saline snow layer, or seawater-filled gaps between/within rafted ice floes. As those impunities show high conductivity, apparent conductivity can be increased by their occurrence. Haas (1998) used a four-layers model, which consists of thin fresh ice layer as snow layer, a seawater-filled gap, a saline ice layer as sea ice and the seawater beneath ice. This gap model can consider the effect of slush layer on the snow/ice interface.

In order to investigate the influence of slush layer, we plot the relationship between σ_a and Z_E for ices with negative freeboard in Fig.10. The ice with negative freeboard can be generally considered to include slush on its top and some of σ_a showed obviously high values of conductivity, the effect of slush was not distinguished clearly in Fig. 10. This result would suggest that the influence of slush is not essential for underestimation of the model curve against the field data. Then we proceed to investigate the influence of the seawater-filled gap within rafted ice floes on the σ_a to Z_E relation.

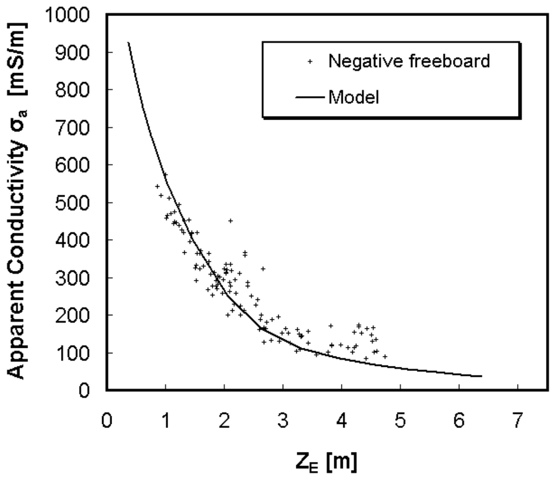

Fig. 10 Z_E-σ_a relationship for negative freeboard ice.

Figure 11 shows the results of classifying into level ice and deformed ice. In this study level ice was classified as a small variance (<10%) with neighboring two forward and two backward drill-hole thicknesses. Thin level ice agrees with model curve very well, but thick ice comes off the curve as well as thick deformed ice. This difference seems to be caused by formation of rafting ice floes. As the maximum thickness of single ice floe was less than 2 m from observation, it is regarded that the thick ice more than 2 m can be formed by at least once rafting process.

To estimate the effect of seawater-filled gaps in the rafted sea ice we used five or seven layers model. We examined thickness ratio of one to one for double or triple rafted floes and also thicknesses Z_G of 0.10 m, 0.20 m and 0.30 m in seawater-filled gaps. These rafted ice models were applied to over 2 m thick ice. For example, when the ice

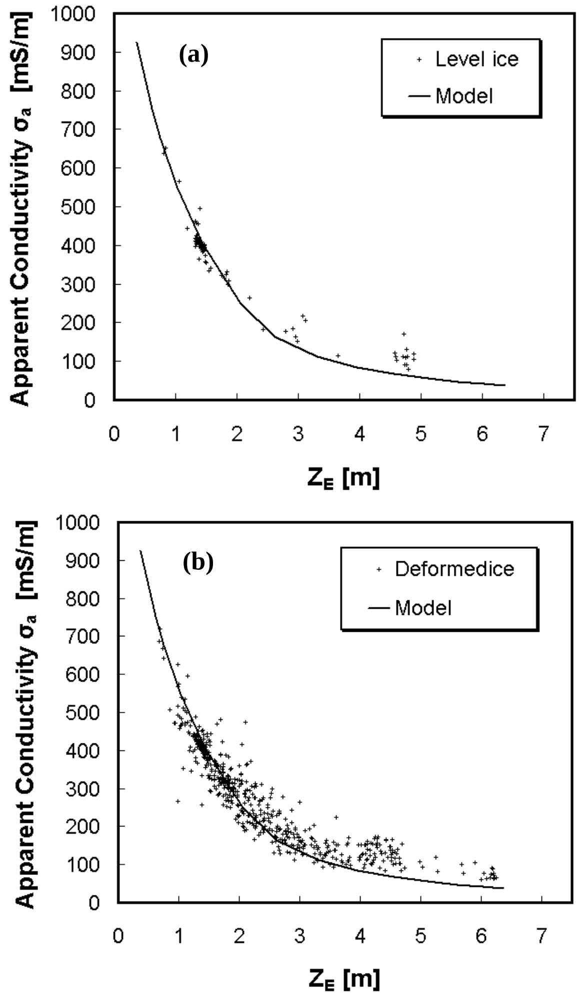

Fig. 11 Z_E-σ_a relationship for negative freeboard ice at Z_L=0.11m.

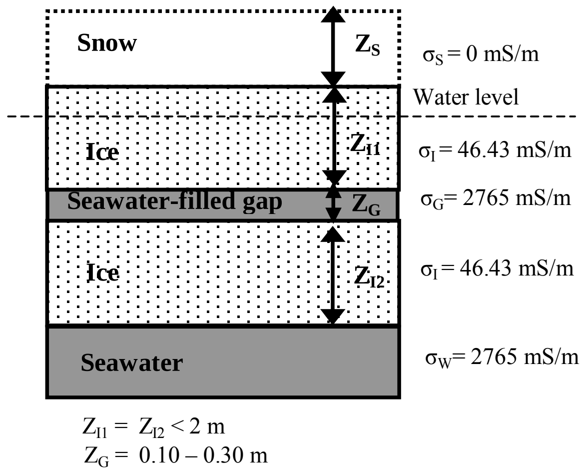

Fig.12 The schematic of a multi-rafted model in this study. The conductivity of seawater-filled gap σ_G was set to be same value of seawater conductivity. Z_{I1} and Z_{I2} are the thickness of each rafted ice

floes. Z_G is the thickness of seawater-filled gap.
thickness is 3 m the model includes a gap between two 1.5 m thick ice floes. When the ice thickness is over 4 m; i.e. the thickness of each single ice floe exceeds 2 m, a triple rafting model is applied. In the other words, the model uses single floe model for 0-2 m, a gap between double floes for 2-4 m and two gaps within triple rafted floes for 4-6 m thick ice. This multi-rafted model is summarized in Fig.12. Here, the conductivity of seawater-filled gap σ_G was set to be same value of seawater conductivity σ_W= 2765 mS/m.

Figure 13 shows a result from the multi-rafted ice model with three different thicknesses of seawater-filled gap versus all averaged in-situ data. The multi-rafted ice model shows the possibility to improve systematic variances in thicker ice over 3.5 m and also to derive a relationship between thick multi-rafted ice and seawater-filled gaps between ice floes. The highest correlation between in-situ and modeled Z_E using multi-rafted model was derived when the thickness of seawater-filled gaps Z_G = 0.10 were used and the correlation coefficient was 0.95. The result of comparison between in-situ and modeled Z_E calculated by the multi-rafted model with Z_G = 0.10 is shown in Fig. 14.

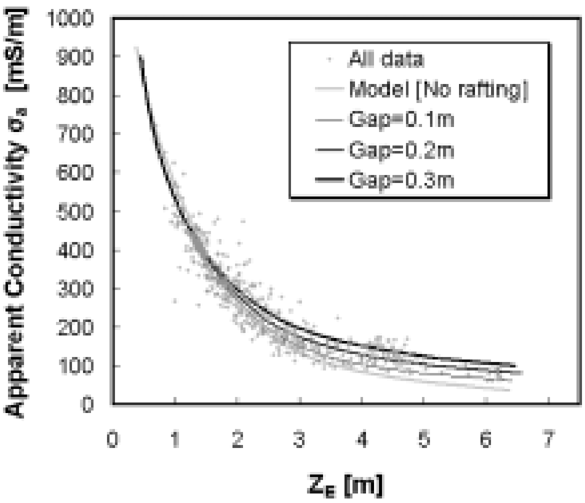

Fig. 13 Rafted ice model results on Z_E-σ_a relationship for all data. Gap means the thickness of seawater-filled gap.

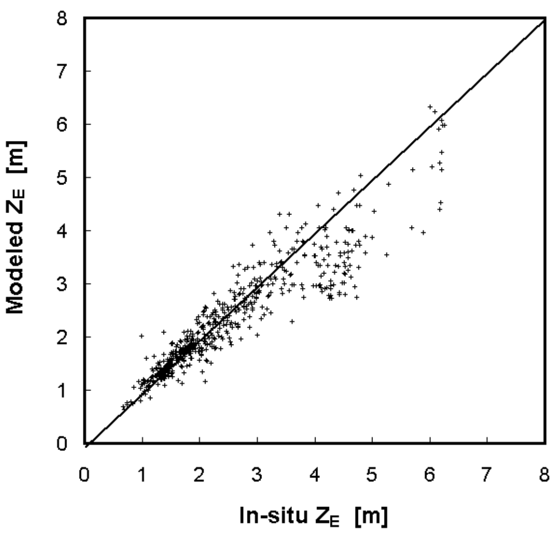

Fig. 14 Comparison between in-situ and modeled Z_E calculated by the multi-rafted ice model.

Figure 15 shows an example of 500 m long transect of in-situ snow and ice thickness with EMI measurement using the ice multi-rafted model with Z_G = 0.10. EMI measurement showed a good agreement in level ice and in slightly deformed ice. On the other hand, a large discrepancy was appeared in highly deformed ice. This problem is considered to be caused by the difference in the sampling interval and the footprint size between in-situ measurement, which was conducted every 2 m in level ice and 1 m in deformed ice, and EMI measurement. The sampling interval of EM-31/ICE was 4 m for level ice and 1 m for deformed ice. Furthermore, as the apparent footprint diameters for VCP mode is about 1.33 times the instrument heights above the interface between ice bottom and seawater as described above, the difference in the spatial resolution also contributes the discrepancy between in-situ data and EMI measurement.

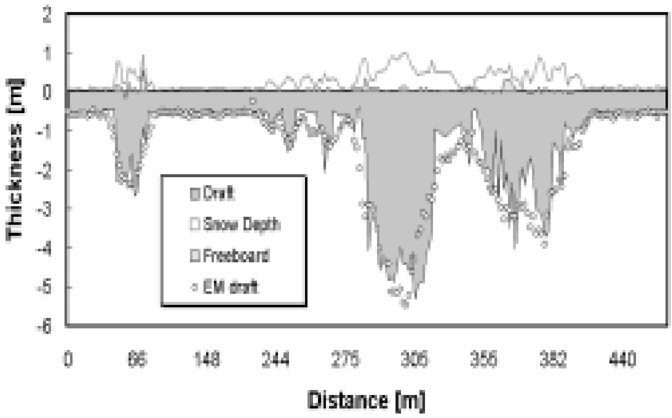

Fig. 15 An example of 500 m long transect of in-situ snow and ice thickness with EMI measurement. Draft, freeboard and snow depth were derived from drill-hole and snow measurement. The white dots mean the ice draft derived from EMI measurement.

CONCLUSIONS

The relationships between ice and snow thickness and apparent conductivity derived from EMI instrument for winter and spring Antarctic sea ice were investigated. For ice with relatively smooth surface and thinner than 2 m, the 1-D three layers model, which is using snow layer, single ice floe layer and seawater layer, showed good agreement within an accuracy of ±10% of in-situ thickness. On the other hand, it is needed to consider seawater-filled gaps between rafting ice floes for thicker ice over about 3.5 m. This multi-rafted ice model showed a good agreement with variances in thickness of thick ice using observed ice and seawater conductivities and critical thickness of single ice floe. Hence EMI measurement using the multi-rafted model with Z_G = 0.10 indicated relevant values to in-situ ice and snow thickness for level ice. The accuracy of EMI measurement will decrease in areas of highly various ice and snow thickness, because spatial resolution depends on thickness.

ACKNOWLEDGEMENTS

We are thankful to the all members of ARISE 2003 led by Dr. Massom, Dr. Allison and Dr. Lytle, who is a principal investigator of this program, a voyage leader and a voyage deputy, respectively. Thanks to the crew of Aurora Australis. Our EMI measurements were carried out in cooperation with Dr. Worby, Dr. Bishop and Mr. Munro. We are also grateful to Dr. Ushio and Dr. Reid for their great helps and valuable advices.

REFERENCES

Archie G. E. (1942), "The electrical resistivity log as an aid in determining some reservoir characteristics", *Trans. Am. Inst. Min. Metall. Pet. Eng*., Vol.146, pp 54-62.

Eicken, H., Tucker III, W. B., and Perovich, D. K. (2001), "Indirect measurements of mass balance of summer Arctic sea ice with an electromagnetic induction technique", *Annals of Glaciol*., Vol.33, pp 194-200.

Frankenstein, G. and Garner, R. (1967), "Equations for determining the brine volume of sea ice from –0.5 °C to –22.9 °C", *J. Glaciology*, Vol.6, pp 943-944.

Haas, C., Gerland, S., Eicken, H. Miller, H. (1997), "Comparison of sea-ice thickness measurements under summer and winter conditions in the Arctic using a small electromagnetic induction device", *Geophysics*, Vol 62, pp 749-757.

Haas, C. (1998), "Evaluation of ship-based electromagnetic-inductive thickness measurements of summer sea-ice in the Bellingshausen and Amundsen Seas, Antarctica", *Cold Regions Sci. Technol*., Vol 27, pp 1-16.

Kovacs, A., Valleau, N. C., and Holladay, J. C. (1987), "Airborne electromagnetic sounding sea-ice thickness and subice bathymetry", *Cold Regions Sci. Technol*., Vol 14, pp 289-311.

Kovacs, A., and Morey, R. M. (1991), "Evaluation of portable electromagnetic induction instrument for measuring sea ice thickness", *CRREL Report*., 91-12, pp 17.

Kovacs, A., C., Holladay, J. C., and Bergeron, Jr. C. J. (1995) "The footprint/altitude ratio for helicopter electromagnetic sounding of sea-ice thickness: Comparison of theoretical and field estimates", *Geophysics*, Vol 60, pp 374-380.

McNeill, J. D. (1980), "Electromagnetic terrain conductivity measurements at low induction numbers" *Geonics Limited Technical Note* TN-6, pp 15.

Multala, J., Hautaniemi, H., Oksama, M., Leppäranta, M., Haapala, J., Herlevi, A., Riska, K. and Lensu, M. (1996), "Airborne electromagnetic surveying of Baltic Sea ice", *Univ. of Helsinki, Dept. of Geophysics. Rep. Ser. Geophys*, 31.

Reid, J. E., Worby, A. P., Vrbancich J. and Munro A. I. S. (2003), "Shipborne electromagnetic measurement of Antarctic sea-ice thickness", *Geophysics*, Vol.68, pp 1537-1546.

Stogryn, A and Desargant, G. J. (1985), "Dielectric properties of brine in sea ice at microwave frequencies", *IEEE Transact. Antenn. Propag*. AP-33(5), pp 523-532.

Uto, S., Shimoda, H. and Izumiyama, K. (2002), "Ship-based sea ice observations in Lützow-Holm Bay, east Antarctica", *Proc 16th IAHR Symp*, Dunedin, New Zealand, pp 218-224.

Worby, A. P., Lytle, V. I. and Massom R. A. (1999), "On the use of electromagnetic induction sounding to determine winter and spring sea ice thickness in the Antarctic", *Cold Regions Sci. Technol*., Vol 29, pp 49-58.